Development of hybrid bioactive nanofibers composed of star Poly(lactic acid) and gelatin by sol–gel crosslinking during the electrospinning process

Karima Belabbes, Matthieu Simon, Christopher Yusef Leon-Valdivieso, Mathilde Massonié, Audrey Bethry, Gilles Subra, Xavier Garric, Coline Pinese

▶ **To cite this version:**

Karima Belabbes, Matthieu Simon, Christopher Yusef Leon-Valdivieso, Mathilde Massonié, Audrey Bethry, et al.. Development of hybrid bioactive nanofibers composed of star Poly(lactic acid) and gelatin by sol–gel crosslinking during the electrospinning process. Nanotechnology, 2023, 34 (48), pp.485701. 10.1088/1361-6528/acf501 . hal-04816934

HAL Id: hal-04816934
https://hal.science/hal-04816934v1

Submitted on 3 Dec 2024

HAL is a multi-disciplinary open access archive for the deposit and dissemination of scientific research documents, whether they are published or not. The documents may come from teaching and research institutions in France or abroad, or from public or private research centers.

L'archive ouverte pluridisciplinaire **HAL**, est destinée au dépôt et à la diffusion de documents scientifiques de niveau recherche, publiés ou non, émanant des établissements d'enseignement et de recherche français ou étrangers, des laboratoires publics ou privés.

Development of hybrid bioactive nanofibers composed of star PLA and gelatin by sol-gel crosslinking during the electrospinning process.

Karima Belabbes [1], Matthieu Simon [2], Christopher Yusef Leon-Valdivieso [1], Mathilde Massonié [1], Audrey Bethry[1], Gilles Subra [2], Xavier Garric [1,3] and Coline Pinese [1]*

[1] Polymers for Health and Biomaterials, IBMM, University of Montpellier, CNRS, ENSCM, Montpellier, France
[2] IBMM peptide, University of Montpellier, CNRS, ENSCM, Montpellier, France
[3] Department of Pharmacy, Nîmes University Hospital, Nimes, France

E-mail: coline.pinese@umontpellier.fr

Received xxxxxx
Accepted for publication xxxxxx
Published xxxxxx

Abstract

The design of a biomimetic scaffold is a major challenge in tissue engineering to promote tissue reconstruction. The use of synthetic polymer nanofibers is widely described as they provide biocompatible matrices whose topography mimics natural extracellular matrix. To closely match the biochemical composition of the extracellular matrix, bioactive molecules such as gelatin are added to the nanofibers to enhance cell adhesion and proliferation. To overcome the rapid solubilization of gelatin in biological fluids and to allow a lasting biological effect, the covalent crosslinking of this macromolecule in the network is crucial. The sol-gel route offers the possibility of gentle crosslinking during shaping but is rarely combined with electrospinning. In this study, we present the creation of PLA/Gelatin hybrid nanofibers by sol-gel route during electrospinning. To enable sol-gel crosslinking, we synthesized star-shaped PLA and functionalized it with silane groups; then we functionalized gelatin with the same groups for their subsequent reaction with the polymer and thus the creation of the hybrid nanonetwork. We evaluated the impact of the presence of gelatin in PLA/Gelatin hybrid nanofibers at different percentages on the mechanical properties, nanonetwork crosslinking, degradation and biological properties of the hybrid nanofibers. The addition of gelatin modulated nanonetwork crosslinking that impacted the stiffness of the nanofibers, resulting in softer materials for the cells. Moreover, these hybrid nanofibers also showed a significant improvement in fibroblast proliferation and present a degradation rate suitable for tissue reconstruction. Finally, the bioactive hybrid nanofibers possess versatile properties, interesting for various potential applications in tissue reconstruction.

Keywords: silylated star PLA; silylated gelatin; hybrid 3D network; bioactive scaffolds; tissue reconstruction

 © xxxx IOP Publishing Ltd

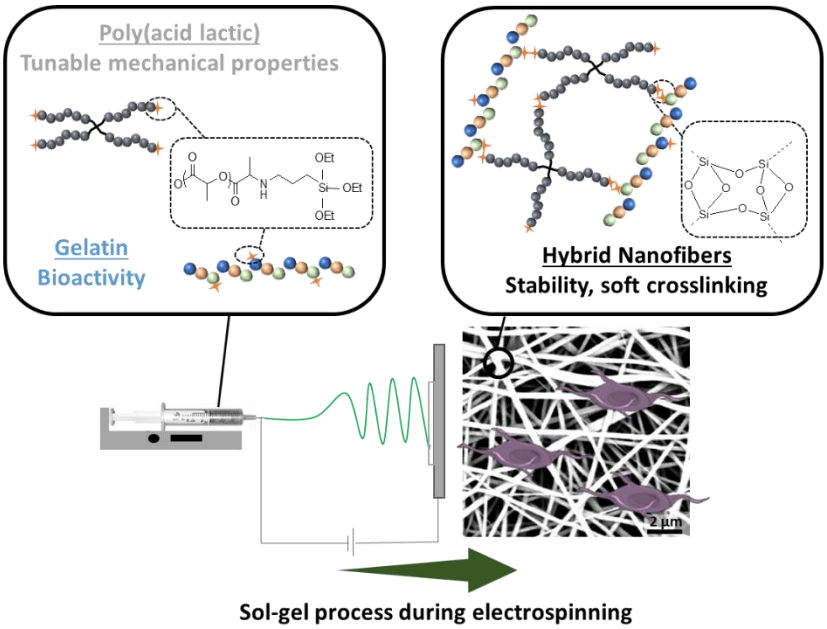

Graphical abstract

 © xxxx IOP Publishing Ltd

1. Introduction

Advances in the field of biomaterials for tissue reconstuction tend to develop structures able to mimic the physical and chemical characteristics of native tissues in order to stimulate the system aiming to recapitulate a normal cellular microenvironment. Electrospinning is a widely used technique that produces polymer-based nanofibrous scaffolds with a surface topography similar to extracellular matrix (ECM) using an electric field [1–4]. Poly(lactic acid)s or PLAs are widely used for the fabrication of nanofibrous scaffolds for tissue reconstruction purposes because of its reproducibility of synthesis, biocompatibility and biodegradability. In particular, PLA nanofibers have interesting mechanical properties and a controllable degradation rate that can be adapted according to the final application [5–7]. Nevertheless, PLA-derived scaffolds are biologically inert and therefore lack cell recognition signals, which may limit the reconstructive performance of the biomaterial [8]. In order to improve the cellular response on nanofibers, ECM components such as gelatin, collagen, laminin and fibronectin [9–13] were introduced in nanofibers to mimic as closely as possible its biochemical composition. In particular, gelatin is an attractive biomolecule due to its biocompatibility, biodegradability, hydrophilicity, widespread availability and low cost [14,15]. This macromolecule is also known to enhance cell adhesion, proliferation, and differentiation [16,17] due to the arginine-glycine-aspartic acid (RGD) segmental motifs on its chains.[18]

The association of gelatin and PLA in hybrid PLA/Gelatin nanofibers shows great promise for tissue reconstruction, combining both structural and chemical characteristics that could mimic ECM [19]. Particularly, grafting gelatin onto the surface of PLA nanofibers is an interesting approach to combine gelatin with PLA. However, this type of surface grafting has limitations, such as the destruction of the porous structure of the nanofiber mat, depending on the power level and processing time [20,21]. The production of electrospun PLA-Gelatin hybrid nanofibers by simple solution mixing has been reported in the literature. However, the low miscibility of the two molecules and their potential phase separation can lead to a deterioration of the mechanical properties of the blends and rapid wear [22]. Additionally, Kim et al demonstrated the degradation of PLA/Gelatin nanofibers at 7 days [19]. Crosslinking for stabilizing macromolecules is then an interesting approach for producing nanofibers that promote tissue reconstruction for a long period of time.

Among the possible cross-linking routes, the sol-gel route is chemoselective and offers soft reaction conditions, protecting the degradation molecules and avoiding impurities [23–26]. This process involves two reaction steps: 1/ hydrolysis of the silane groups attached to PLA and gelatin to form silanols and 2/ condensation of the functions to form siloxane bonds. Although sol-gel cross-linking of macromolecules has already been used to form films [27] or gels for 3D printing [28], there is no work on the formation of nanofibres using this method.

In this study, we produced nanofibers composed of an hybrid nanonetwork of PLA providing mechanical properties and gelatin providing bioactivity properties. The novelty of this project lies in the challenge of covalently crosslinking modified versions of PLA and gelatin during electrospinning via the sol-gel process for the first time. To enable the crosslinking reaction during the electrospinning process, we functionalized four-armed star PLA and gelatin with silane groups. We investigated the impact of incorporating gelatin into the star PLA network on the mechanical properties, crosslinking efficiency and degradation. We then performed proliferation tests on these hybrid nanofibers to verify the biological properties provided by the addition of gelatin. The modularity of the system and the results obtained illustrate the interest of these nanofibers for an application in tissue reconstruction.

2. Materials and methods

2.1 Materials

Pentaerythritol, diethylene glycol (DEG), Tin (II) 2-ethylhexanoate ($Sn(Oct)_2$, 95%), 3-(Triethoxysilyl)propyl isocyanate (ICPTES), N,N-diisopropylethylamine (DIEA), gelatin B from bovine skin (G9391-100G), toluene, heptane, N,N-dimethylformamide, tetrahydrofuran, dichloromethane (DCM), diethyl ether, trifluoroethanol, trifluoroacetic acid (TFA) and hydrochloric acid (37%) (1M in Methanol) were furnished by Sigma-Aldrich (St Quentin Fallavier, France). D,L-lactide was purchased from Corbion (Gorinchem, The Netherlands). PrestoBlue® assay (A13262) and Clariostar plate reader (A13626) were received from Introgen.

 © xxxx IOP Publishing Ltd

2.2 Synthesis of tetra-triethoxysilane functionalized PLA (PLA-4arms-PTES)

A star-shaped PLA with 4 arms of 25 $kg.mol^{-1}$ and 5 $kg.mol^{-1}$ were synthesized by ring-opening polymerization, following a previously described procedure.[29] For the synthesis of PLA-4arms-5k: D,L-lactide (30 g, 6 mmol, 14 eq), pentaerythritol as a multifunctional initiator (1.09 g, 0.22 mmol, 4 eq) and $SnOct_2$ as a catalyst (0.039 g, 0.96 mmol, 0.16 eq) were put in a flask 2 h under vacuum and sealed. After polymerization at 120 °C for 5 days, the resulting polymer was solubilized in dichloromethane and then purified in cold heptane (4 °C). PLA-4arms-25k was obtained using the same procedure by varying the ratio (L,D-lactide/pentaerythritol). After vacuum drying, the molecular weight of PLA-4arms was determined by ^{1}H-NMR from the ratio of the methylene protons of the pentaerythritol to the methyne proton of the lactic unit.

^{1}H-NMR (400 MHz, $CDCl_3$) δ (ppm) = 5.15 (m, C**H**CH_3); 4.34 (m, C**H**CH_3OH); 4.14 (s, CC**H**$_2$O); 3.5 (s, CC**H**$_2$OH); 1.54 (m, CHC**H**$_3$).

Then, both PLA-4arms (PLA-4arms-25k and PLA-4arms-5k) were functionalized using a previously described procedure.[30] PLA-4arms-5k (5 g, 1.1 mmol) was placed under anhydrous conditions and vacuum for 4 h before being solubilized by adding 100 mL of anhydrous toluene. The reaction was initiated by the addition of IPTES (1.63 g, 6.6 mmol, 6 eq) and $SnOct_2$ (0.178 g, 0.44 mmol, 0.4 eq) under inert gas (stirring, 75 °C, OVN). The functionalized polymer was precipitated with cold heptane (4 °C) and subsequently vacuum dried. The number of IPTES group on all arms of PLA-4arms was obtained from ^{1}H-NMR spectra using the ratio of signals from the methyne proton of the lactic unit (δ = 5.1 ppm) and the methylene proton bound to tri-ethoxysilane (δ = 0.6 ppm).

^{1}H-(400 MHz, $CDCl_3$) δ (ppm)= 5.15 (m, C**H**CH_3); 4.14 (s, CC**H**$_2$O); 3.83 (m, OC**H**$_2$$CH_3$); 3.5 (s, CC**H**$_2$OH); 3.17 (m, NHC**H**$_2$); 1.54 (m, CHC**H**$_3$); 1.2 (m, OCH_2C**H**$_3$); 0.64–0.54 (m, CH_2C**H**$_2$ Si).

2.3 Gelatin silylation (Gelatin-PTES)

Gelatin B solution was prepared at a concentration of 0.02 $g.mL^{-1}$ in anhydrous DMSO and stirred at 55 °C for 2 h. The resulting solution was dried using sodium sulfate and then centrifuged at 3000 rpm for 10 min to collect the supernatant, considered as a 2% (w/v) solution. The conservation of this solution was carried out under inert atmosphere and in the dark.

Then, gelatin was silylated with functionalization degree of 40% or 100% (Gelatin-PTES-40 and Gelatin-PTES-100) using an already described protocol.[31] Briefly, Gelatin-PTES were obtained by adding ICPTES (5 eq or 0.5 eq for Gelatin-PTES-40 and Gelatin-PTES-100 respectively) and N, N-Diisopropylethylamine (DIEA, 10 eq) to 30 mL of a 2% (w/v) gelatin solution. The reaction was carried out under inert atmosphere and at room temperature for 1 h. Then, to purify the silylated gelatin, the reaction solution was added dropwise, with vigorous stirring, into 240 mL of diethyl ether/tetrahydrofuran (40/60, v/v). Addition of 50 mL of diethyl ether precipitated the gelatin which was recovered by centrifugation (3000 rpm for 10 min) followed by 3 washes with diethyl ether. The obtained powder was ground, dried under vacuum and conserved in an inert atmosphere in the dark.

^{1}H-(600MHz, DMSO-d6) δ (ppm)= 0.5 (m, R-C**H**$_2$-Si$(OEt)_3$); 2.7 (m, $CH_2CH_2CH_2$C**H**$_2$$NH_2$); 5.8 (m, R-N**H**-CO-N**H**-R).

A fluorescent silylated gelatin (Gelatin-PTES-FITC) was also prepared to visualize the gelatin in hybrid electrospun nanofibers. Briefly, FITC (0.1 eq/NH_2 of gelatin) and N,N-Diisopropylethylamine (DIEA, 10 eq) was added in 2% (w/v) gelatin solution and stirred for 1 h at RT before IPTES (5 eq) was added and stirred for 1 h at RT. The final product was recovered using the same previous precipitation protocol.

^{1}H-(600MHz, DMSO-d6) δ (ppm)= 0.5 (m, R-C**H**$_2$-Si$(OEt)_3$); 2.7 (m, $CH_2CH_2CH_2$C**H**$_2$$NH_2$); 5.8 (m, R-N**H**-CO-N**H**-R); 6.5 (m, C**H**CHOH).

2.4 Electrospinning

To prepare nanofibers without gelatin (PLA_{-Si-XL}), we solubilized 0.1 g of PLA-4arms-5k-PTES, 0.05 g of PLA-4arms-25k-PTES and 0.05 g of LinearPLA200k in 1 mL of TFE. We then activated the sol-gel process by adding 10 µL of HCL (0.1 M in ethanol) under stirring for 60 sec. The solution was put into a 21-G syringe and placed in a syringe pump (KDS100, KD Scientific) for which a flow rate of 0.5 $mL.h^{-1}$ was set. To initiate the electrospinning

 © xxxx IOP Publishing Ltd

process, a voltage of 15 kV was applied to the system. The nanofibers were then recovered on a flat collector that was 15 cm distanced from the syringe needle.

Hybrid Polymer/Gelatin nanofibers were obtained by introducing Gelatin-PTES-40 or Gelatin-PTES-100 into the polymer solution at different weight ratios: 0.2, 2 and 20% (w/w), corresponding to 0.42, 4.2 and 42 mg of gelatin respectively for $(PLA/G_{40}\text{-}0.2\%)_{\text{-Si-XL}}$, $(PLA/G_{40}\text{-}2\%)_{\text{-Si-XL}}$ and $(PLA/G_{40}\text{-}20\%)_{\text{-Si-XL}}$. The solubilizations of the Gelatin-PTES-40 and Gelatin-PTES-100 was performed in 1.3 mL of TFE by ultrasound for 30 min and 2 h respectively at constant stirring. After activattion of the sol-gel process by adding 10 µL of HCL for 60 sec, we electrospun the solutions using the same parameters as described above at 25 ± 1 °C with a relative humidity of 48 ± 3%.

To assess the impact of crosslinking on the properties of the nanofibers, we made control nanofibers composed of a silylated but uncrosslinked polymer or and gelatin ($PLA_{\text{-Si}}$ and $(PLA/G_{40}\text{-}2\%)_{\text{-Si}}$) under the same conditions except that crosslinking was not triggered by the addition of HCL. Furthermore, to determine the impact of gelatin crosslinking in the network, we made nanofibers composed of crosslinked PLA and non-silylated gelatin ($PLA_{\text{-Si-XL}}/G_{40}\text{-}2\%$).

2.5 Characterization methods

2.5.1 Chemical characterization

Size exclusion chromatography (SEC) was carried out with an LC-200AD Prominence Shimadzu system instrumented using a PLgel MIXED-C guard column (Agilent, 5 µm, 50 × 7.5 mm), two PLgel MIXED-C columns (Agilent, 5 µm, 300 × 7.5 mm), and a RID-20A refractive index signal. Poly(ethylene glycol) was used as a calibration standard. The obtained polymers were solubilized in THF at 10 $mg.mL^{-1}$. The resulting solution was then filtered with a Millipore membrane (0.45 µm) and 200 µL of this solution was pumped into the system with a flow rate of 1 $mL.min^{-1}$.

The ^{1}H-NMR spectra of samples with gelatin were acquired on a Bruker 600 MHz spectrometer equipped with a cryoprobe and pulsed field gradients. The gelatin samples were prepared by dissolving 15 mg in DMSO-d6 while the polymers were dissolved in deuterated chloroform.

2.5.2 Nano-structure characterization

For Scanning Electron Microscopy (SEM), the resulting nanofibers were sputter coated with 10 nm thick gold using an accelerating voltage of 15 kV in a Quorum SC7620 Sputter Coat. The fibers diameter was measured using Image J (https://imagej.nih.gov/ij/download.html (accessed on 12th of April 2021)) (number of fibers for each condition = 40).

EVOS® microscope (EVOS™ XL Core Imaging System, Thermo Fisher Scientific, cat. no. AMEX1000) was employed for visualization of nanofibers. All samples were analyzed using the exact same parameters to ensure accurate comparison between samples.

2.6 Gel fraction

The obtained nanofibers layers were cut into strips (10 × 30 mm, n=4) and immersed after weighing (initial weight W_i) in 3 mL of trifluoroethanolat under constant stirring for 3h. The solutions were then centrifuged (3000 rpm for 10 min) to separate the insoluble and soluble fractions. After isolation and vacuum-drying, the insoluble and soluble fractions were weighed ($W_{\text{insoluble}}$ and W_{soluble}, respectively) and the gel fraction calculated with the following equation:

Gel fraction (%) = $(W_{\text{insoluble}}/W_i) \times 100$

2.7 Mechanical properties

Uniaxial tensile tests were performed on rectangular shaped samples (3 x 1 cm, n=4) with an Instron 3344 test system at a rate of 5 $mm.min^{-1}$ using a 500 N load cell. The Young's modulus (E, MPa) as well as the strain maximal at break (ε_{max}, %) were measured at 25 ± 1 °C. The Young's modulus was calculated using the initial linear part of the stress-strain curve.

 © xxxx IOP Publishing Ltd

2.8 Degradation

Electrospun scaffolds (10 x 30 mm, 7.5 ± 3 mg) were weighed (mi=initial mass) and then immersed in 6 mL of PBS (pH=7.4) at 37 °C under constant stirring. Samples were removed from PBS at different time points and their mass loss, water uptake and gel fraction were evaluated in quadruplicates. The water uptake and mass loss were calculated as follows :

Water uptake (%) = $((m_w-m_d)/m_d)$ x100

Mass loss (%) = $((m_i-m_d)/m_i)$ x100

Where m_w is the hydrated mass of the scaffolds and m_d is mass after vacuum drying overnight.

The gel fractions were evaluated following protocols described previously.

2.8 Proliferation assays

2.8.1 Cell culture

NHDF (Normal Human Dermal Fibroblasts) (Thermofisher C0135C, Batch 2186199, passage 5) were cultured in 500 mL DMEM with 5 mL glutamax (1% stabilized glutamine), 50 mL horse serum, and 100 $U.mL^{-1}$ penicillin and streptomycin 100 $\mu g.mL^{-1}$.

2.8.2 Proliferation test

Disks of nanofibers with a diameter of 2 cm were sterilized by UV-C irradiation (λ = 254 nm, 2.5 min on each side, 80 W) and fixed in untreated 24-well plate using O-rings; NHDFs were then seeded on top of the nanofibers at $8x10^4$ cells per well and placed at 37 °C and 5% CO_2. Cell counts were performed after 1, 5, 11 and 13 days using PrestoBlue™ according to the provider's protocol. Briefly, PrestoBlue™ reagent was mixed with cell culture medium in a 1:10 volume ratio; 100 mL of this mix was pipetted into each well and incubated in the dark for 40 min at 37 °C. A fluorescence intensity reading was performed using a CLARIOstar® microplate reader (wavelength: excitation 558 nm, emission 590 nm; INVITROGEN). After each measurement, the supernatant was replaced with fresh medium to continue the cell culture until the end of the study.

2.9 Statistical Analysis

Statistical tests were performed by R software version 3.5.2. Significance was assessed by the nonparametric Kruskall-Wallis test with repeated measures, followed by Dunn's posttest. Values of $p < 0.05$ were considered significant.

3. Results and discussion

The production of nanofibers composed of a combination of natural biomaterial such as gelatin with degradable synthetic polymers is highly interesting for biomedical application. Firstly, the polymers aid in the fabrication of homogeneous nanofibers with mechanical strength; secondly, the nanofibers mimic the microstructural topography of the ECM; and thirdly, they possess appropriate chemical and biological cues that might favor the reconstruction process, mainly coming from the gelatin moiety. In general, the current studies are based on a simple mixture of PLA with gelatin in the solution to be electrospun, leading to too rapidly degraded nanofibers [19]. Our strategy is based on the covalent grafting of gelatin onto four-armed star-shaped PLAs to create a stable hybrid PLA/Gelatin nanofibrous matrix employing sol-gel process and electrospinning in a single step. This approach is based on the modification of PLA and gelatin by triethoxysilane groups.

3.1 Synthesis of tetra-triethoxysilane functionalized PLA (PLA-4arms-PTES)

To increase the number of reactive functions available for the nanonetwork creation, we used polymers with a 4-arms star architecture. PLA-4arms-25k and PLA-4arms-5k were obtained by polymerizing L,D-lactide on 4-arm

 © xxxx IOP Publishing Ltd

pentaerythritol in the presence of $Sn(Oct)_2$, following a ring-opening mechanism as shown in Figure 1A. As shown in Figure 1B, ^{1}H-NMR analysis confirmed the polymerization of lactide on pentaerythritol. The molecular weight, calculated by the ratio of the methylene of pentaerythritol at 4.14 ppm to the methyne of the lactic acid units at 5.15 ppm, were 4,550 and 22,600 g.mol^{-1} for PLA-4arms-5k and PLA-4arms-25k which was very close to the theoretical molecular weight (Figure 1C). Moreover, the absence of a signal at 4.33 ppm shows that all the hydroxy functions of the pentaerythritol have been used and thus confirmed the star architecture. The SEC analysis shows a monomodal profile and a narrow distribution in SEC (Đ), which is consistent for such a synthesis [32]. This indicates that the polymerization reaction resulted in a high degree of uniformity in the polymer chain length and molecular weight distribution. This is a desirable outcome for the synthesis of polymers, as it can result in improved mechanical properties and other performance characteristics in the final product.

Then, the PLA-4arms were functionalized with IPTES groups to form PLA-4arms-PTES. This was achieved through the reaction of isocyanate groups with PLA terminal hydroxyls in presence of $Sn(Oct)_2$ leading to the formation of urethane bonds. The number of PTES grafted groups on the PLA-4arms were calculated by ^{1}H-NMR from the ratio of signals between the methyne proton of lactic units at 5.1 ppm and the triethoxysilane methylene protons at 0.6 ppm. It was 3.85 and 4 on PLA-4arms-5k-PTES and PLA-4arms-25k-PTES respectively, corresponding to a degree of functionalization of 94.5% and 100% (Figure 1C).

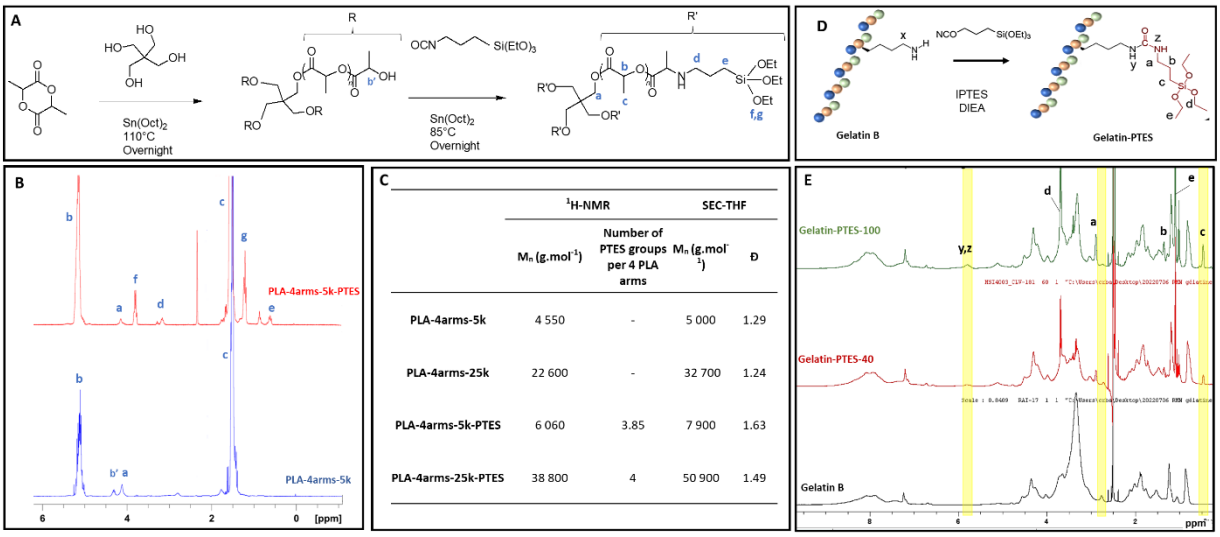

	^{1}H-NMR		SEC-THF	
	M_n (g.mol^{-1})	Number of PTES groups per 4 PLA arms	M_n (g.mol^{-1})	Đ
PLA-4arms-5k	4 550	-	5 000	1.29
PLA-4arms-25k	22 600	-	32 700	1.24
PLA-4arms-5k-PTES	6 060	3.85	7 900	1.63
PLA-4arms-25k-PTES	38 800	4	50 900	1.49

Figure 1. Synthesis of tetra-functionalized PLA and functionalized Gelatin: (A) Synthesis of PLA-4arms-PTES reaction scheme; (B) ^{1}H-NMR spectrum of PLA-4arms-5k and PLA-4arms-5k-PTES; (C) ^{1}H-NMR and SEC characterizations of PLA-4arms-PTES; (D) Gelatin silylation reaction; (B) ^{1}H-NMR spectrum of Gelatin, Gelatin-PTES-40 and Gelatin-PTES-100.

3.2 Gelatin-PTES synthesis

Gelatin was modified to Gelatin-PTES by reacting the isocyanate groups of ICPTES with the amines of the lysine side chain to form urea bonds under anhydrous basic conditions (Figure 1D). ^{1}H-NMR analyses confirmed the coupling of PTES to gelatin. The decrease (gelatin-PTES-40) or even the disappearance (gelatin-PTES-100) of the proton signals corresponding to the free amines of gelatin (2.7 ppm) confirmed the formation of urea bonds (5.8 ppm) between the free amines of gelatin and the ICPTES molecules (Figure 1E). The functionalization rate was determined by calculating the ratio of the methylene protons of the PTES groups to the protons of the lysine side chain. The results showed a functionalization rate of 100% for gelatin-PTES-100 and 40% for gelatin-PTES-40.

3.3 Production and characterization of hybrid PLA-4arms-PTES/Gelatin-PTES nanofibers

 © xxxx IOP Publishing Ltd

In a previous work, we successfully combined sol-gel crosslinking of silylated polymers with the electrospinning process to create nanofibers composed of a silylated star PLA network [29]. To ensure stable bioactivity over time and to modulate the mechanical properties of the nanofibers, we mixed PLA-4arms-PTES and Gelatin-PTES to create nanofibers composed of a PLA/Gelatin hybrid nanonetwork. To initiate the sol-gel pathway, the molecules were solubilized in a common solvent, TFE, and the acid hydrolysis of the PTES silane groups was triggered in the syringe prior to electrospinning. During the formation of the nanofibers, condensation of the formed silanol groups occurred, leading to the creation of siloxane bonds between the macromolecules and the generation of the hybrid nanonetwork.

Polymeric nanofibers without gelatin ($PLA_{\text{-Si-XL}}$) as well as hybrid nanofibers containing increasing quantity of gelatin (PLA/G_{100}-0.2%)$_{\text{-Si-XL}}$, (PLA/G_{100}-2%)$_{\text{-Si-XL}}$, (PLA/G_{100}-5%)$_{\text{-Si-XL}}$ and (PLA/G_{40}-20%)$_{\text{-Si-XL}}$ were obtained using this process. The resulting nanofibers were found homogeneous in terms of size and distribution (Figure 2A). To confirm the incorporation of Gelatin-PTES into the nanofibers, we conducted an experiment in which different amounts of a fluorophore-tagged version of Gelatin-PTES (Gelatin-PTES-FITC) were added to the electrospun PLA-4arms-PTES solution. Fluorescence microscopy images showed that the fluorescent gelatin was homogeneously distributed in the nanofibers, regardless of the amount added (Figure 2B). Moreover, we can observe an increase of the fluorescence intensity with the amount of Gelatin-PTES-FITC incorporated in the nanofibers. It has been reported that during electrospinning a rearrangement of the molecules often occurs [33]. To determine whether gelatin was present on the surface of the nanofibers, we studied the ratio of nitrogen (main component of the gelatin chain) to carbon by elemental analysis of the different nanofibers produced with Gelatin-PTES. The nitrogen/carbon ratio increased as the polymer/gelatin mass ratio increased (0.2%, 2 and 20%) which confirms the presence of gelatin on the surface of the nanofibers, available to the cells (Figure 2C). These analyses also revealed that gelatin was present at the surfaces of nanofibers whether or not gelatin was crosslinked to the network: nanofibers composed of a non-crosslinked networks ((PLA/G_{40}-2%)$_{\text{-Si}}$), or a network where only PLA was crosslinked and not gelatin ($PLA_{\text{-Si-XL}}/G_{40}$-2%) have the same N/C ratio as fully crosslinked networks (PLA/G_{100} -2%)$_{\text{-Si-XL}}$.

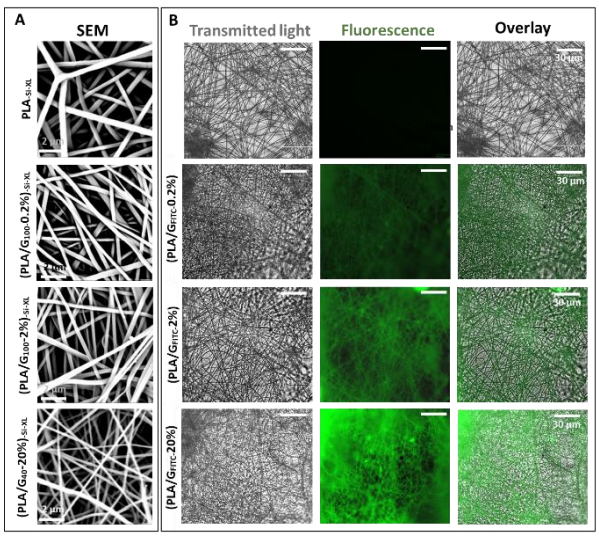

D

Nanofibers	Fiber diameters (µm)	Gel Fraction (%)	Mechanical properties	
			E (MPa)	ε_f (%)
$PLA_{\text{-Si-XL}}$	0.33 ± 0.09	61.1 ± 5.6	76.5 ± 21	24.9 ± 1.1
$PLA_{\text{-Si}}$	0.63 ± 0.22	-	22.9 ± 2.6	2.18 ± 0.3
(PLA/G_{100}-0.2%)$_{\text{-Si-XL}}$	0.29 ± 0.06	62.3 ± 17	70.0 ± 8.03	27.8 ± 6.3
(PLA/G_{100} -2%)$_{\text{-Si-XL}}$	0.33 ± 0.10	30.1 ± 8.1	64.3 ± 11	0.25 ± 0.1
(PLA/G_{100} -5%)$_{\text{-Si-XL}}$	0.29 ± 0.07	15.9 ± 1.1	45.3 ± 7.3	0.19 ± 0.1
(PLA/G_{40}-20%)$_{\text{-Si-XL}}$	0.23 ± 0.04	52.1 ± 9.3	12.2 ± 4.14	3.05 ± 1.2
(PLA/G_{40}-2%)$_{\text{-Si-XL}}$	0.26 ± 0.38	43.7 ± 24	65.3 ± 2.1	26.2 ± 15
(PLA/G_{40}-2%)$_{\text{-Si}}$	0.24 ± 0.05	-	17.9 ± 10	2.8 ± 0.4
$PLA_{\text{-Si-XL}}/G_{40}$-2%	0.36 ± 0.08	66.1 ± 8.1	71.3 ± 15	15.2 ± 3.9

Figure 2. Hybrid Polymer/Gelatin nanofibers crosslinked during electrospinning : (A) SEM images of nanofibers composed of nanonetworks that contain 0 ($PLA_{\text{-Si-XL}}$), 0.2 ((PLA/G_{100}-0.2%)$_{\text{-Si-XL}}$), 2 ((PLA/G_{100} -2%)$_{\text{-Si-XL}}$) and 20% of gelatin ((PLA/G_{40}-20%)$_{\text{-Si-XL}}$); (B) Fluorescence images of nanofibers that contain Gelatin-FITC à 0, 0.2, 2 and 20%; (C) Elemental analysis (N/C ratio) of hybrid nanofibers using energy dispersive x ray spectroscopy ; (D) Hybrid nanofibers diameters, gel fraction and mechanical properties.

The complexity of combining sol-gel and electrospinning lies in successfully creating siloxane bonds during the polymer jet travel from the syringe to the collector. Previous works have shown the development of this process to obtain highly crosslinked star polymer nanofibers [29]. Therefore, we studied the impact of gelatin incorporation on the crosslinking rate of the nanonetworks by comparing the gel fractions of PLA/Gelatin hybrid nanofibers with $PLA_{\text{-Si-XL}}$ nanofibers (Figure 2D). While the introduction of 0.2% gelatin did not significantly affect the gel fraction

 © xxxx IOP Publishing Ltd

of the nanonetworks, the gel fraction decreased with the increase of the amount of gelatin in the mixture, from 61% for $PLA_{\text{-Si-XL}}$ nanofibers to 30.1% and 15.9% for $(PLA/G_{100}\text{-}2\%)_{\text{-Si-XL}}$ and $(PLA/G_{100}\text{-}5\%)_{\text{-Si-XL}}$. This decrease can be explained by the presence of gelatin which is a large molecule able to limit the formation of siloxane bonds (Si-O-Si) between the polymers. Moreover, we could hypothesize that the gelatin underwent self-cross linking, forming a larger molecule and thus reducing the crosslinking of the network. This hypothesis was confirmed by the impossibility to electrospun Polymer/Gelatin solutions containing a percentage of gelatin-PTES-100 higher than 5% due to the formation of insoluble crosslinked gelatin bulk after the activation of the sol-gel route. For this reason, we used a less crosslinked gelatin (Gelatin-PTES-40) with the aim of increasing the gelatin concentration to 20% in the nanofibers. Not surprisingly, by limiting the possibility of intramolecular crosslinking, the introduction of gelatin-PTES-40 increased the gel fractions to 52.1% and 43.7% for $(PLA/G_{40}\text{-}20\%)_{\text{-Si-XL}}$ and $(PLA/G_{40}\text{-}2\%)_{\text{-Si-XL}}$ respectively. The introduction of gelatin as well as the changes in the crosslinking rates of the nanonetworks had direct consequences on the mechanical properties of the nanofiber mats. The Young's modulus, which reflects the stiffness of the nanofibers, was decreased from 76.5 MPa for the $PLA_{\text{-Si-XL}}$ nanofibers to 45.3 and 12.2 MPa for the $(PLA/G_{100}\text{-}5\%)_{\text{-Si-XL}}$ and $(PLA/G_{40}\text{-}20\%)_{\text{-Si-XL}}$ nanofibers respectively. Consequently, the strain at break followed the same trend. The mechanical properties of the crosslinked nanofibers ($(PLA/G_{40}\text{-}2\%)_{\text{-Si-XL}}$) showed the importance of the crosslinking between the macromolecules of the network compared to macromolecules physical entanglement: While the uncrosslinked nanofibers young's modulus ($(PLA/G_{40}\text{-}2\%)_{\text{-Si}}$) was 17.9MPa, the crosslinking increased the stiffness value to 65.3MPa ($(PLA/G_{40}\text{-}2\%)_{\text{-Si-XL}}$). However, the lack of significant difference between the gel fractions and the young's modulus of the nanofibers composed of crosslinked Star-PLA and gelatin nanonetworks ($(PLA/G_{40}\text{-}2\%)_{\text{-Si-XL}}$) vs. a crosslinked Star-PLA and uncrosslinked gelatin nano networks ($PLA_{\text{-Si-XL}}/G_{40}\text{-}2\%$) showed that the crosslinking of the gelatin had little impact on the properties of the nanonetworks. In addition to the crosslinking rate, the presence of the gelatin molecule itself had a direct impact on the young's modulus, since the $(PLA/G_{40}\text{-}2\%)_{\text{-Si-XL}}$ and $(PLA/G_{40}\text{-}20\%)_{\text{-Si-XL}}$ nanofibers have very different young's moduli (65.3 and 12.2MPa) for the same crosslinking rate.

3.4 Hybrid nanofibers degradation

The interest of having degradable nanofibers for biomedical use is well established. However, the presence time of the nanofibers must be sufficient to support regeneration and provide bioactivity throughout this process. We have studied the *in vitro* degradation of hybrid nanofibers. The loss of mass of the samples is represented in Figure 3A which showed the sample weight as function of time. The loss of mass of hybrid samples were visible from 15 days; after 30 days the losses were slight for samples containing 0.2 and 2% gelatin (8%) and much more important for samples containing 20% gelatin (31%). Usually, the *in vitro* degradation of PLA nanofibers is done by penetration of water into the nanonetwork. Surprisingly, the increase in the percentage of gelatin did not significantly influence the penetration of water into the samples with water uptakes between 55 and 85% for all quantities of gelatin (Figure 3B), except for $PLA_{\text{-Si}}$ whose water uptake has fallen due to the absence of si-o-si bonding and then to the loss of nanofibers morphology. The water infiltrated into the nanonetwork seemed to trigger the reaction of unreacted functions during the nanofiber fabrication process as shown by the increase of the gel fractions (Figure 3C) just after immersion in the degradation medium ($PLA_{\text{-Si-XL,}}$ $(PLA/G_{40}\text{-}0.2\%)_{\text{-Si-XL,}}$ and $(PLA/G_{40}\text{-}2\%)_{\text{-Si-XL}}$). The aqueous catalysis of silane functions is well described in the literature as well as the water-ageing of this kind of materials [34,35]. According to our results, this new link formation occurred in the first three days, and did not interfere with the gradual decrease of the gel fraction over the following 30 days.

Finally, the water infiltrated into the network can initiate the hydrolysis of the ester functions composing the PLA. Gel fraction of the $PLA_{\text{-Si-XL}}$ samples (Figure 3C) drops during the degradation time, while the samples did not lose mass and did not undergo major morphological changes (Figure 3D). It suggests that the hydrolysis of the ester bonds has already started but that the oligomers generated were not small enough to be solubilized in the degradation medium.

Despite this beginning of hydrolysis, the morphology of the nanofibers containing 0.2 and 2% gelatin did not change over time. However, pores corresponding to degradation were visible from 3 days on the nanofibers containing 20% gelatin. This change in morphology became more pronounced with increasing degradation time. The total loss of morphology of $PLA_{\text{-si}}$ and $(PLA/G_{40}\text{-}2\%)_{\text{-Si}}$ nanofibers after 3 days of degradation showed the importance of crosslinking in the nanofibers morphology conservation.

 © xxxx IOP Publishing Ltd

Finally, the formation of the nanonetwork maintained the nanofiber form for at least 30 days despite the onset of degradation. This persistence was higher than that of the uncrosslinked PLA/gelatin nanofibers [19] and allows us to consider the possibility of supporting tissue reconstruction over this period of time.

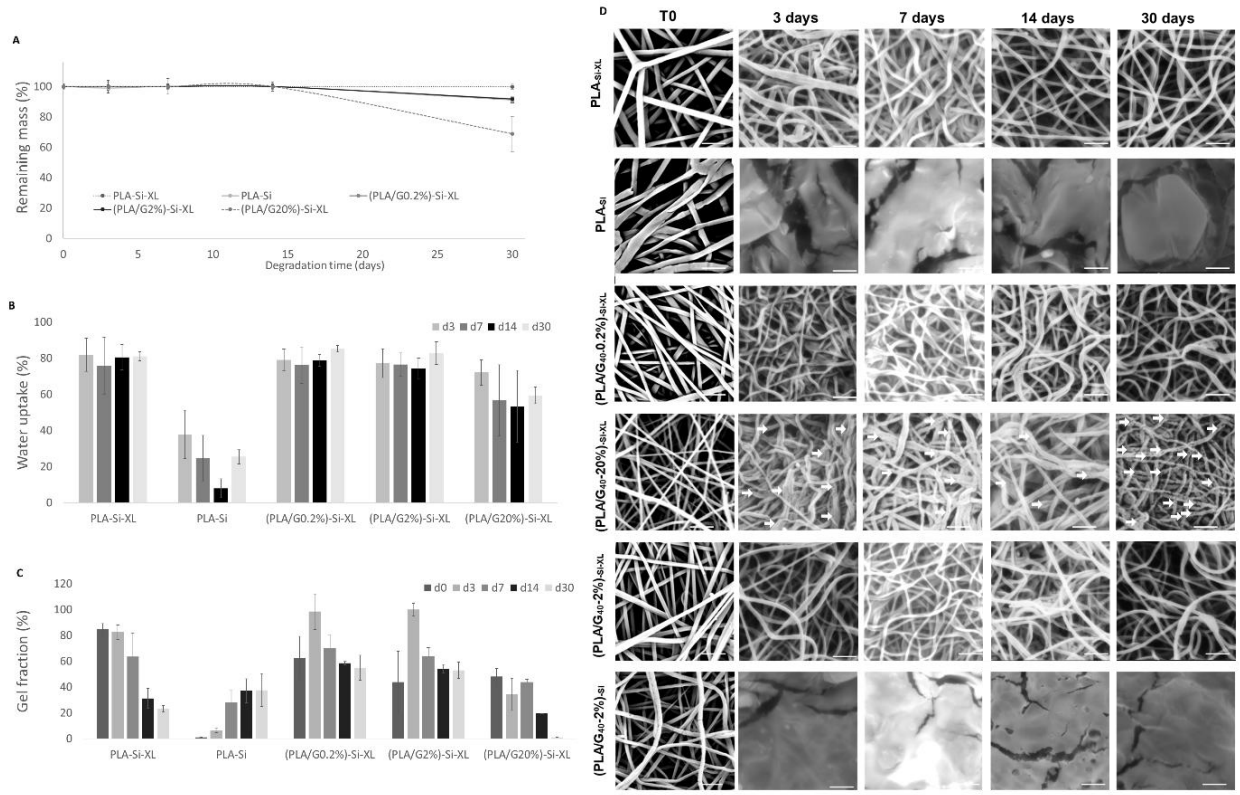

Figure 3. Hybrid Polymer/Gelatin (PLA/G40) nanofibers *in vitro* degradation over 30 days: (A) Remaining mass of sample after immersion in PBS; **(B) Water uptake of nanofibers during degradation time; (C) Gel fraction of nanonetworks during degradation time; (D) SEM images that showed the hybrid nanofibers morphologies loss (evidenced by the white arrows).**

3.5 Cells proliferation assays

To demonstrate the suitability of $(PLA/G)_{\text{-Si-XL}}$ hybrid nanofibers for medical applications, we studied the proliferation of NHDFs which are, among others, one of the main drivers to produce a new extracellular matrix (Figure 4A).

The objective of introducing gelatin into the polymer nanofibers was to improve their biological properties. While cells did not proliferate on nanofibers without gelatin ($PLA_{\text{-Si-XL}}$), it was found that $(PLA/G_{100}\text{-}2\%)_{\text{-Si-XL}}$, $(PLA/G_{100}\text{-}5\%)_{\text{-Si-XL}}$ and $(PLA/G_{40}\text{-}20\%)_{\text{-Si-XL}}$ nanofibers significantly improved the proliferation of NHDFs up to 13 days. Surprisingly, the proliferation was not improved with increasing the amount of gelatin in the nanofibers. However, the addition of gelatin in the nanofibers clearly improved cell proliferation and allowed the cells to spread on the surface of the nanofibers (Figure 4B).

The improved proliferation on silylated nanofibers was likely due to the presence of gelatin, especially the presence of a bioactive RGD segment responsible for the improvement of RGD cell response [18] such as cell adhesion and growth [36,37].

Although it has been shown previously that the presence of PTES groups on PLA does not interfere with the proliferation of L929 [30] we aimed to confirm this on NHDFs. We therefore produced nanofibers with non-functionalized-PLA and non-silylated gelatin. The proliferation of NHDF was dramatically reduced on these samples because of their fast degradation due to of the absence of crosslinking between the macromolecules.

 © xxxx IOP Publishing Ltd

These results showed the interest of the creation of PLA/Gelatin networks for a biomedical application due to 1/ the presence of gelatin with interesting biological properties and 2/ the formation of a crosslinked networks which retains the structure of the network and its biological properties for at least 13 days. The hybrid scaffolds obtained by our study constitute a microenvironment that physically and biochemically mimics the ECM, providing a matrix for tissue reconstruction with a wide range of applications depending on these mechanical properties.

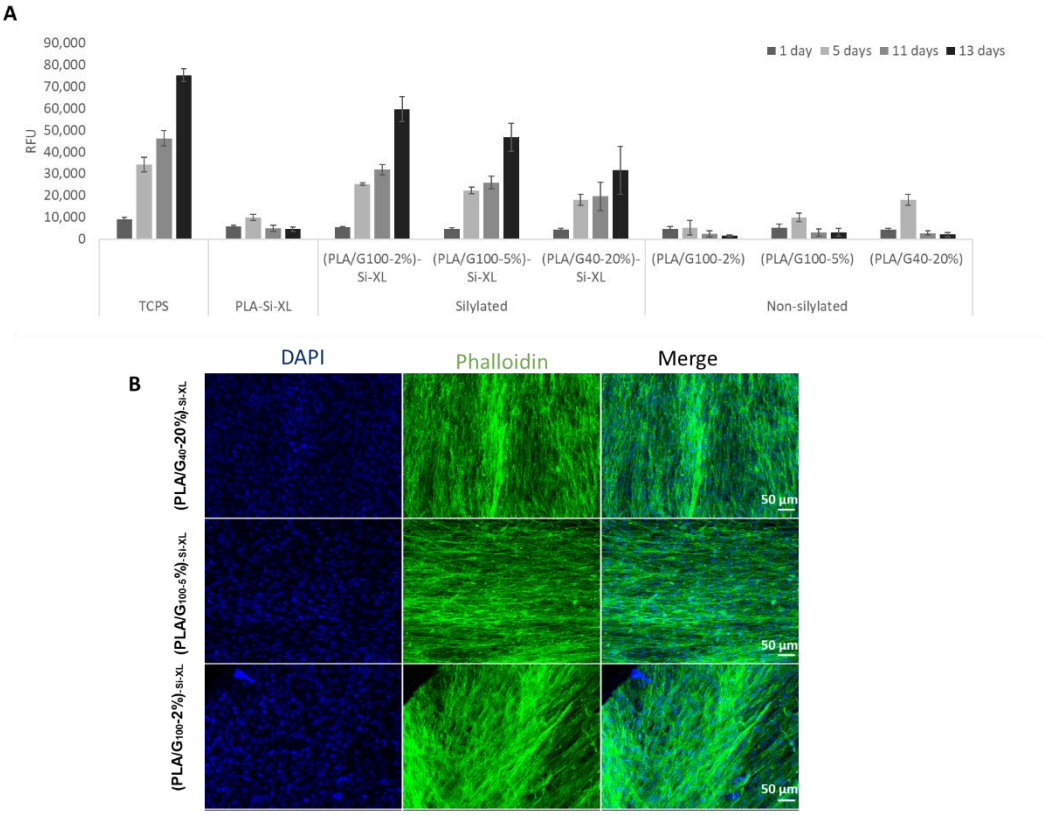

Figure 4. (A) *In vitro* NHDF proliferation on (PLA_{-Si-XL}), (PLA/G_{100}-2%)$_{-Si-XL}$, (PLA/G_{100}-5%)$_{-Si-XL}$ and (PLA/G_{40}-20%)$_{-Si-XL}$ in comparison with TCPS and non-silylated nanofibers as control (B) Immunostaing images of NHDF after 13 days on hybrid nanofibers.

4. Conclusion

In conclusion, electrospun PLA nanofibers have shown great potential as a three-dimensional support for tissue reconstitution due to their biocompatibility and biodegradability. However, to impart bioactivity to these nanofibers, the covalent incorporation of a bioactive molecule seems to be an effective approach. In this work, we have for the first-time crosslinked gelatin with PLA by sol-gel process during electrospinning to create bioactive hybrid nanofibers. These hybrid nanofibers offer several advantages over traditional PLA nanofibers, including their ability to mimic the microstructural topography of the extracellular matrix,, the possibility to tailormechanical properties by the polymers/gelatin ratio according to different clinical needs and the presence of appropriate chemical and biological cues that might favor the reconstruction process, mainly coming from the gelatin moiety. These hybrid nanofibers were found to be less rigid, and their degree of crosslinking could be tailored by increasing the percentage of functionalized gelatin. The incorporation of silylated gelatin resulted in higher fibroblast proliferation compared to PLA nanofibers without gelatin or with non-crosslinked gelatin. Overall, our strategy offers a promising way to produce scalable, bioactive PLA-based biomaterials for tissue engineering applications. Future research in this area may involve exploring different bioactive molecules that can be incorporated into the hybrid nanofibers to further enhance their biological properties.

 © xxxx IOP Publishing Ltd

Acknowledgements

Karima Belabbes's PhD was supported by the Algerian Ministry of Higher Education and Scientific Research (MESRS) (Scholarship of excellence). Polymer characterizations were performed using Synbio3 platform supported by GIS IBISA. We acknowledge the CARTIGEN platform (IRMB, CHU, Montpellier, France) for scanning electron microscopy facilities access.

References

[1] Biazar E. Application of polymeric nanofibers in soft tissues regeneration: Nanofibers in Medical Sciences. Polym Adv Technol 2016;27:1404–12. https://doi.org/10.1002/pat.3820.
[2] Liao S, Li B, Ma Z, Wei H, Chan C, Ramakrishna S. Biomimetic electrospun nanofibers for tissue regeneration. Biomed Mater 2006;1:R45–53. https://doi.org/10.1088/1748-6041/1/3/R01.
[3] Dahlin RL, Kasper FK, Mikos AG. Polymeric Nanofibers in Tissue Engineering. Tissue Engineering Part B: Reviews 2011;17:349–64. https://doi.org/10.1089/ten.teb.2011.0238.
[4] Jiang T, Carbone EJ, Lo KW-H, Laurencin CT. Electrospinning of polymer nanofibers for tissue regeneration. Progress in Polymer Science 2015;46:1–24. https://doi.org/10.1016/j.progpolymsci.2014.12.001.
[5] Santoro M, Shah SR, Walker JL, Mikos AG. Poly(lactic acid) nanofibrous scaffolds for tissue engineering. Advanced Drug Delivery Reviews 2016;107:206–12. https://doi.org/10.1016/j.addr.2016.04.019.
[6] Kumbar SG, Nukavarapu SP, James R, Nair LS, Laurencin CT. Electrospun poly(lactic acid-co-glycolic acid) scaffolds for skin tissue engineering. Biomaterials 2008;29:4100–7. https://doi.org/10.1016/j.biomaterials.2008.06.028.
[7] Gangolphe L, Leon-Valdivieso CY, Nottelet B, Déjean S, Bethry A, Pinese C, et al. Electrospun microstructured PLA-based scaffolds featuring relevant anisotropic, mechanical and degradation characteristics for soft tissue engineering. Materials Science and Engineering: C 2021;129:112339. https://doi.org/10.1016/j.msec.2021.112339.
[8] Engstrand T. Biomaterials and Biologics in Craniofacial Reconstruction. Journal of Craniofacial Surgery 2012;23:239. https://doi.org/10.1097/SCS.0b013e318241c0f4.
[9] Wang J, Sun B, Tian L, He X, Gao Q, Wu T, et al. Evaluation of the potential of rhTGF- β3 encapsulated P(LLA-CL)/collagen nanofibers for tracheal cartilage regeneration using mesenchymal stems cells derived from Wharton's jelly of human umbilical cord. Materials Science and Engineering: C 2017;70:637–45. https://doi.org/10.1016/j.msec.2016.09.044.
[10] Li M, Guo Y, Wei Y, Macdiarmid A, Lelkes P. Electrospinning polyaniline-contained gelatin nanofibers for tissue engineering applications. Biomaterials 2006;27:2705–15. https://doi.org/10.1016/j.biomaterials.2005.11.037.
[11] Chiara G, Letizia F, Lorenzo F, Edoardo S, Diego S, Stefano S, et al. Nanostructured Biomaterials for Tissue Engineered Bone Tissue Reconstruction. IJMS 2012;13:737–57. https://doi.org/10.3390/ijms13010737.
[12] Junka R, Valmikinathan CM, Kalyon DM, Yu X. Laminin Functionalized Biomimetic Nanofibers for Nerve Tissue Engineering. J Biomat Tissue Engng 2013;3:494–502. https://doi.org/10.1166/jbt.2013.1110.
[13] Chantre CO, Campbell PH, Golecki HM, Buganza AT, Capulli AK, Deravi LF, et al. Production-scale fibronectin nanofibers promote wound closure and tissue repair in a dermal mouse model. Biomaterials 2018;166:96–108. https://doi.org/10.1016/j.biomaterials.2018.03.006.
[14] Yung CW, Wu LQ, Tullman JA, Payne GF, Bentley WE, Barbari TA. Transglutaminase crosslinked gelatin as a tissue engineering scaffold. J Biomed Mater Res 2007;83A:1039–46. https://doi.org/10.1002/jbm.a.31431.
[15] Chen J-P, Su C-H. Surface modification of electrospun PLLA nanofibers by plasma treatment and cationized gelatin immobilization for cartilage tissue engineering. Acta Biomaterialia 2011;7:234–43. https://doi.org/10.1016/j.actbio.2010.08.015.
[16] Echave MC, Burgo LS, Pedraz JL, Orive G. Gelatin as Biomaterial for Tissue Engineering. CPD 2017;23. https://doi.org/10.2174/0929867324666170511123101.
[17] Loth T, Hötzel R, Kascholke C, Anderegg U, Schulz-Siegmund M, Hacker MC. Gelatin-Based Biomaterial Engineering with Anhydride-Containing Oligomeric Cross-Linkers. Biomacromolecules 2014;15:2104–18. https://doi.org/10.1021/bm500241y.
[18] Su K, Wang C. Recent advances in the use of gelatin in biomedical research. Biotechnol Lett 2015;37:2139–45. https://doi.org/10.1007/s10529-015-1907-0.
[19] Kim H-W, Yu H-S, Lee H-H. Nanofibrous matrices of poly(lactic acid) and gelatin polymeric blends for the improvement of cellular responses. Journal of Biomedical Materials Research Part A 2008;87A:25–32. https://doi.org/10.1002/jbm.a.31677.
[20] Dufay M, Jimenez M, Degoutin S. Effect of Cold Plasma Treatment on Electrospun Nanofibers Properties: A Review. ACS Appl Bio Mater 2020;3:4696–716. https://doi.org/10.1021/acsabm.0c00154.
[21] Safinia L, Wilson K, Mantalaris A, Bismarck A. Through-thickness plasma modification of biodegradable and nonbiodegradable porous polymer constructs. J Biomed Mater Res 2008;87A:632–42. https://doi.org/10.1002/jbm.a.31731.
[22] Alhalawani AMF, Curran DJ, Boyd D, Towler MR. The role of poly(acrylic acid) in conventional glass polyalkenoate cements. Journal of Polymer Engineering 2016;36:221–37. https://doi.org/10.1515/polyeng-2015-0079.
[23] Schubert U. Chemistry and Fundamentals of the Sol-Gel Process. In: Levy D, Zayat M, editors. The Sol-Gel Handbook, Weinheim, Germany: Wiley-VCH Verlag GmbH & Co. KGaA; 2015, p. 1–28. https://doi.org/10.1002/9783527670819.ch01.

 © xxxx IOP Publishing Ltd

[24] Mackenzie JD. Applications of the sol-gel process. Journal of Non-Crystalline Solids 1988;100:162–8. https://doi.org/10.1016/0022-3093(88)90013-0.
[25] Danks AE, Hall SR, Schnepp Z. The evolution of 'sol–gel' chemistry as a technique for materials synthesis. Mater Horiz 2016;3:91–112. https://doi.org/10.1039/C5MH00260E.
[26] Bergna HE, editor. The Colloid Chemistry of Silica. vol. 234. Washington DC: American Chemical Society; 1994. https://doi.org/10.1021/ba-1994-0234.
[27] Arsenie LV, Pinese C, Bethry A, Valot L, Verdie P, Nottelet B, et al. Star-poly(lactide)-peptide hybrid networks as bioactive materials. European Polymer Journal 2020;139:109990. https://doi.org/10.1016/j.eurpolymj.2020.109990.
[28] Echalier C, Levato R, Mateos-Timoneda MA, Castaño O, Déjean S, Garric X, et al. Modular bioink for 3D printing of biocompatible hydrogels: sol–gel polymerization of hybrid peptides and polymers. RSC Adv 2017;7:12231–5. https://doi.org/10.1039/C6RA28540F.
[29] Belabbes K, Pinese C, Leon-Valdivieso CY, Bethry A, Garric X. Creation of a Stable Nanofibrillar Scaffold Composed of Star-Shaped PLA Network Using Sol-Gel Process during Electrospinning. Molecules 2022;27:4154. https://doi.org/10.3390/molecules27134154.
[30] Arsenie LV, Pinese C, Bethry A, Valot L, Verdie P, Nottelet B, et al. Star-poly(lactide)-peptide hybrid networks as bioactive materials. European Polymer Journal 2020;139:109990. https://doi.org/10.1016/j.eurpolymj.2020.109990.
[31] Simon M, Maumus M, Legrand B, Sole L, Dufaud M, Mehdi A, et al. Gelatin modified with alkoxysilanes (GelmSi) forms hybrid hydrogels for bioengineering applications. Biomaterials Advances 2023;147:213321. https://doi.org/10.1016/j.bioadv.2023.213321.
[32] Michalski A, Brzezinski M, Lapienis G, Biela T. Star-shaped and branched polylactides: Synthesis, characterization, and properties. Progress in Polymer Science 2019;89:159–212. https://doi.org/10.1016/j.progpolymsci.2018.10.004.
[33] Morel A, C. Oberle S, Ulrich S, Yazgan G, Spano F, J. Ferguson S, et al. Revealing non-crystalline polymer superstructures within electrospun fibers through solvent-induced phase rearrangements. Nanoscale 2019;11:16788–800. https://doi.org/10.1039/C9NR04432A.
[34] Bao X, Liu F, He J. Mechanical properties and water-aging resistance of glass ionomer cements reinforced with 3-aminopropyltriethoxysilane treated basalt fibers. J Mech Behav Biomed Mater 2021;116:104369. https://doi.org/10.1016/j.jmbbm.2021.104369.
[35] Antico E, Leutzsch M, Wessel N, Weyhermüller T, Werlé C, Leitner W. Selective oxidation of silanes into silanols with water using [MnBr(CO) 5] as a precatalyst. Chemical Science 2023;14:54–60. https://doi.org/10.1039/D2SC05959B.
[36] Wu S, Ni S, Jiang X, Kuss MA, Wang H-J, Duan B. Guiding Mesenchymal Stem Cells into Myelinating Schwann Cell-Like Phenotypes by Using Electrospun Core–Sheath Nanoyarns. ACS Biomater Sci Eng 2019;5:5284–94. https://doi.org/10.1021/acsbiomaterials.9b00748.
[37] Wang Y, Wu S, Kuss MA, Streubel PN, Duan B. Effects of Hydroxyapatite and Hypoxia on Chondrogenesis and Hypertrophy in 3D Bioprinted ADMSC Laden Constructs. ACS Biomater Sci Eng 2017;3:826–35. https://doi.org/10.1021/acsbiomaterials.7b00101.

 © xxxx IOP Publishing Ltd